Ultrafast Intermolecular Hydrogen Bond Dynamics in the Excited State of Fluorenone

Vaishali Samant, Ajay K. Singh, G. Ramakrishna, Hirendra N. Ghosh, Tapan K. Ghanty, and Dipak K. Palit*

Radiation Chemistry & Chemical Dynamics Division, Bhabha Atomic Research Center, Mumbai 400089, India

Received: February 17, 2005; In Final Form: July 30, 2005

Steady-state fluorescence and time-resolved absorption measurements in pico- and femtosecond time domain have been used to investigate the dynamics of hydrogen bond in the excited singlet (S_1) state of fluorenone in alcoholic solvents. A comparison of the features of the steady-state fluorescence spectra of fluorenone in various kinds of media demonstrates that two spectroscopically distinct forms of fluorenone in the S_1 state, namely the non-hydrogen-bonded (or free) molecule as well as the hydrogen-bonded complex, are responsible for the dual-fluorescence behavior of fluorenone in solutions of normal alcoholic solvents at room temperature (298 K). However, in 2,2,2-trifluoroethanol (TFE), a strong hydrogen bond donating solvent, emission from only the hydrogen-bonded complex is observed. Significant differences have also been observed in the temporal evolution of the absorption spectroscopic properties of the S_1 state of fluorenone in protic and aprotic solvents following photoexcitation using 400 nm laser pulses. An ultrafast component representing the solvent-induced vibrational energy relaxation (VER) process has been associated with the dynamics of the S_1 state of fluorenone in all kinds of solvents. However, in protic solvents, in addition to the VER process, further evolution of the spectroscopic and dynamical properties of the S_1 state have been observed because of repositioning of the hydrogen bonds around the carbonyl group. In normal alcohols, two different kinds of hydrogen-bonded complex of the fluorenone−alcohol system with different orientations of the hydrogen bond with respect to the carbonyl group and the molecular plane of fluorenone have been predicted. On the other hand, in TFE, formation of only one kind of hydrogen-bonded complex has been observed. These observations have been supported by theoretical calculations of the geometries of the hydrogen-bonded complexes in the ground and the excited states of fluorenone. Linear correlation between the lifetimes of the equilibration process occurring because of repositioning of the hydrogen bonds and Debye or longitudinal relaxation times of the normal alcoholic solvents establish the fact that, in weakly hydrogen bond donating solvents, the hydrogen bond dynamics can be described as merely a solvation process. Whereas, in TFE, hydrogen bond dynamics is better described by a process of conversion between two distinct excited states, namely, the non-hydrogen-bonded form and the hydrogen-bonded complex.

1. Introduction

Intermolecular hydrogen bonding is a site-specific local interaction between hydrogen donor and acceptor molecules. Hydrogen bonding is a fundamental element of chemical structure and reactivity of water, proteins, and the DNA building blocks of life.[1−4] The nature of the hydrogen bond in solution is of particular interest and has been probed by diverse experimental and theoretical methods. However, we do not have much information on structural and relaxation dynamics of the hydrogen bond after electronic excitation of molecules that are part of an intermolecular hydrogen bond. Upon photoexcitation of molecules in solution, the dipole moment of the molecules changes, sometimes significantly, and this necessitates a major reorganization of the surrounding solvent molecules around the newly created molecular dipole to minimize the total energy of the molecule−solvent system. This process of reorganization of the solvent molecules is popularly known as solvation.[5−10] Here, the local interaction between the solute and the first solvation cell is very important, and obviously, hydrogen bonding has a very important role to play.[9−15] To understand the dynamics of chemical reactions at the molecular level, one needs to study the microscopic motion of the solvent molecules engaged in such specific solute−solvent interactions.[16−18] The nature of coupling between the solute and the solvent molecules also governs the rate and mechanism of the transfer of vibrational energy from the excited solute to the solvent bath.[19−21]

In a rigid molecular system, in which the difference in dipole moment between the ground and the excited states is significantly large, the S_1 state attains the intramolecular charge transfer (ICT) character upon photoexcitation. In such cases, solvation plays an important role in the relaxation dynamics of the excited state.[22] In the case of aprotic solvents, the dipole−dipole interaction between the excited state and the solvent molecules is the main driving force for the orientational motions of the solvent molecules around the solute molecule.[5−7,16,23] However, in the case of protic or hydrogen bond donating solvents, such as alcohols or amines, in addition to dipole−dipole interaction, orientational motion of the solvent molecules may also be affected by specific interactions via intermolecular hydrogen bonds, in case the solute molecule provides efficient hydrogen bond accepting sites, such as CO or NO_2 group.[13−15,24] In some cases, the solute molecules in the ground state form strongly hydrogen-bonded complexes with the solvent molecules. Upon photoexcitaion, as a consequence of significant

* Corresponding author: e-mail dkpalit@apsara.barc.ernet.in; Tel 91-22-25595091; Fax 91-22-25505151/25519613.

10.1021/jp050848f CCC: $30.25
Published on Web 09/08/2005

difference in charge distribution in the higher-energy electronic states of the solute molecules, the solute and the solvent molecules, engaged in the formation of hydrogen bonds, need to reorganize themselves. We define this process as the hydrogen bond dynamics, and this controls the excited-state dynamics in a significant way.[13,14] Dynamics of hydrogen bond occur on ultrafast time scales mainly set by vibrational motions of the hydrogen donor and acceptor groups. Experiments in the femtosecond time regime have shown the potential to monitor the microscopic features of the hydrogen bond dynamics in real time.[13−15]

We find that fluorenone is an ideal molecule for studying the hydrogen bond dynamics because of several reasons. First, primary photophysics of fluorenone has been well studied because fluorenone exhibits some rather unique spectroscopic and photophysical properties that have made it the subject of several investigations.[25−35] These studies have led to a reasonably consistent picture of the degradative energy flow pattern in fluorenone following light absorption. Fluorenone, like all other molecules with an active ⟩C═O group, has two kinds of excited states, namely nπ^* and $\pi\pi^*$. In these kind of molecules, hydrogen bonding and polarity are the key factors in controlling the pathways of energy dissipation following electronic excitation.[35−37] Change in the relative positions of these two types of levels due to change in solvent characteristics influences the rates of transitions from the singlet to the triplet levels by virtue of El-Sayed's rule.[38] Although the lowest excited nπ^* and $\pi\pi^*$ singlet levels are lying very close to each other in nonpolar solvents, the energies of these states are solvent shifted depending on the polarity of the solvents, so that the $\pi\pi^*$ state becomes the lowest excited singlet (S_1) state in polar solvents. This factor controls the reactivity of the singlet state as well as the yield of the triplet state by controlling the intersystem crossing rate.[30,39,40] The lifetimes of the S_1 state of fluorenone have been reported to be much longer in polar aprotic solvents than those in nonpolar as well as in polar protic solvents.[41]

Second, another major aspect of the photophysics of fluorenone, which has been well studied, is quenching of the excited states via hydrogen-bonding interactions.[35,42] Fluorenone forms an intermolecular hydrogen-bonded complex with alcohols in the ground state. In addition, both the S_1 and T_1 states are dynamically quenched due to hydrogen-bonding interaction with the alcoholic solvent molecules.[35] In this process, the hydrogen bond acts as an efficient accepting mode for radiationless deactivation processes. Photoexcitation results in significant changes in the spatial charge distribution around the oxygen atom depending on the kind of transition, i.e., whether it is nπ^* or $\pi\pi^*$. Hence, this prompts the major changes in the orientation of the solvent molecule directly attached to the carbonyl oxygen as well as the solvent molecules linked with the former via the hydrogen-bonding network structure of the solvent.

Third, fluorenone is a planar molecule with a rigid framework, and hence, no other relaxation process, such as conformational or configurational relaxation, than the relaxation process arising due to solvent motions is important in the S_1 state. Finally, the change of dipole moment ($\Delta\mu = 2.2$ D) upon photoexcitation of fluorenone to its S_1 state is not very large.[43] Hence, the difference in the spectroscopic properties between the Franck−Condon (FC) state and the relaxed excited state following dipolar solvation is expected not to be very significant. However, we may expect a significant change in the spectroscopic properties of the excited state due to hydrogen bond dynamics via the specific interaction between the carbonyl group and the molecules of the protic solvents. Since fluorenone is very weakly fluorescent, the transient absorption spectroscopic technique should be a very useful tool to reveal the role of hydrogen bond dynamics in the excited-state relaxation processes of fluorenone.[41] In this paper, we report the ultrafast dynamics of the relaxation processes taking place in the S_1 state of fluorenone in different kinds of solvents, such as aprotic and protic (or alcoholic), and show that hydrogen bond dynamics really does play an important role in the relaxation process of the S_1 state of fluorenone in protic solvents.

2. Experimental Section

Fluorenone, obtained from Thomas-Becker sensitizers' kit, has been purified by recrystallization from methanol. Solvents of spectroscopic grade (Spectrochem, India) were used without further purification. Steady-state absorption spectra were recorded on a Shimadzu model UV-160A spectrophotometer. Fluorescence spectra, which were corrected for wavelength dependence of the instrument response, were recorded using a Hitachi model 4010 spectrofluorimeter. High-purity grade nitrogen gas (Indian Oxygen, purity >99.9%) was used to deaerate the samples. All experiments were carried out at room temperature (298 K) unless specified otherwise. The emission spectra in rigid matrices at 77 K were recorded by freezing the sample solutions, which were taken in a round quartz tube of 4 mm diameter, in liquid nitrogen put in a quartz dewar.

The time-resolved transient absorption spectra have been recorded with 35 ps time resolution using a picosecond laser flash-photolysis apparatus, the details of which have been described in ref 44. Briefly, the third harmonic output (355 nm, 5 mJ) from an active passive mode-locked Nd:YAG laser (Continuum, model 501-C-10) providing 35 ps pulses was used for excitation and the continuum (400−950 nm) probe pulses were generated by focusing the residual fundamental in a 10 cm cell containing a H_2O/D_2O mixture. The probe pulses were delayed with respect to the pump pulses using an 1 m long linear translation stage, and the transient absorption signals at different probe delays (up to 6 ns) were recorded by an optical multichannel analyzer (Spectroscopic Instruments, Germany) interfaced to an IBM-PC. The zero delay position has been assigned to that when the probe light reaches the sample just after the end of the pump pulse.

Relaxation processes in the sub-100 ps time domain were measured using a femtosecond pump−probe transient absorption spectrometer, which used a laser system supplied by CDP-Avesta, Russia, The pulses of 50 fs duration and 6 nJ energy per pulse at 800 nm were obtained from a self-mode-locked Ti−sapphire laser oscillator, which was pumped by a 5 W diode-pumped solid-state laser. These pulses were amplified to generate 70 fs laser pulses of about 300 μJ energy at a repetition rate of 1 kHz using the chirped pulse amplification (CPA) technique. The optical amplifier consisted of a pulse stretcher, a multipass Ti:sapphire amplifier pumped by an intracavity frequency-doubled Nd:YAG laser (6 W, 1 kHz), and a pulse compressor. Pump pulses at 400 nm were generated for excitation of the samples by frequency-doubling of one part of the 800 nm output of the amplifier in a 0.5 mm thick BBO crystal, and the other part of the amplifier output was used to generate the white light continuum (470−1000 nm) probe in a 2 mm thick sapphire plate. The direction of polarization of the pump beam was fixed at the magic angle. Excitation energy was kept below 10 μJ/pulse, and the repetition rate of the pump beam was maintained at 500 Hz using a chopper. The sample solutions were kept flowing through a quartz cell of 1 mm path length. The decay dynamics at a particular wavelength region

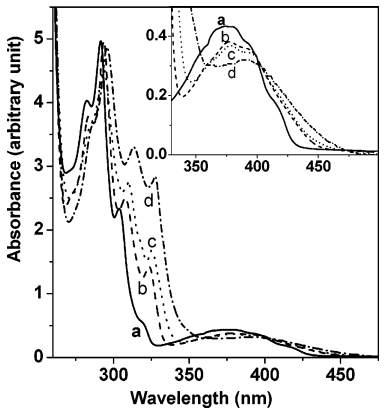

Figure 1. Steady-state absorption spectra of the ground electronic state of fluorenone in cyclohexane (a), acetonitrile (b), methanol (c), and TFE (d).

(10 nm width) was selected using a pair of interference filters placed in front of the photodiodes to monitor the integrated intensity of the reference probe beam and the probe beam passing through the excited zone. The outputs of these photodiodes were routed through the boxcar integrators to an ADC and computer for calculation of the optical density of the transient species at a particular delay time. The delay time between the pump and probe pulses was varied by using a stepper motor driven single-axis linear motion stage (with 0.1 μm/step resolution), which was put on the path of the pump beam. The overall time resolution of the absorption spectrometer was determined to be about 120 fs by measuring the ultrafast growth of excited-state absorption (ESA) at different wavelengths in the 470−1000 nm region following photoexcitation of tetraphenylprophyrin in benzene. These temporal profiles were also used to correct the effects of temporal dispersion on the time-resolved spectra through the adjustments of the positions of the zero delay between the pump and probe pulses at different wavelengths. The temporal profiles recorded using different probe wavelengths were fitted with up to three exponentially decaying or growing components by iterative deconvolution method using an $sech^2$ type instrument response function with fwhm of 120 fs.

3. Results

3.1. Steady-State Absorption and Fluorescence Studies. Before investigating the dynamical properties of the hydrogen bond in fluorenone−alcohol systems, we planned to investigate the steady-state spectroscopic properties of fluorenone. This strengthened our understanding and arguments regarding the relaxation behavior of the system in the same kind of media, in which the dynamical properties have been investigated. Figure 1 shows the electronic absorption spectra of fluorenone in the 270−500 nm region in four nonaqueous solvents, namely cyclohexane, acetonitrile, methanol, and 2,2,2-trifluoroethanol (TFE). The spectroscopic properties of the lower lying electronically excited states of fluorenone have been well-investigated earlier.[25,39,45] In this wavelength region, the electronic absorption spectrum recorded in each of these solvents consists of a few well-resolved absorption peaks. From the detailed analysis of the vibrational structures and solvent effects on the position of the absorption peaks, Kuboyama suggested that the total absorption spectrum of fluorenone in this region consists of three absorption bands, namely in the 270−300, 300−350, and 350−500 nm regions, originating from three different $\pi \rightarrow \pi^*$ kinds of electronic transitions.[45]

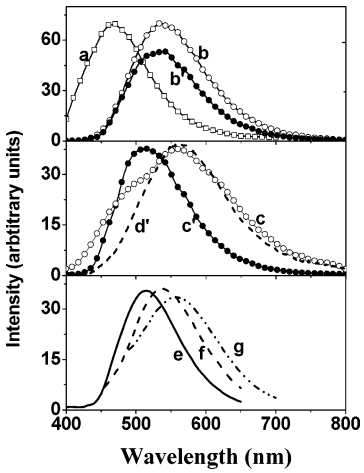

Figure 2. Steady-state fluorescence spectra of fluorenone in cyclohexane at 298 K (a); in acetonitrile at 298 K (b) and 77 K (b′); in methanol at 298 K (c) and 77K (c′); in TFE at 77 K (d′); in dimethylformamide (e), dimethylformamide (50%) + formamide (50%) mixture (f), and formamide (g) at 298 K.

Figure 2 shows the emission spectra of fluorenone in solvents of different classes, recorded at two different temperatures, i.e., in solution at room temperature (298 K) and in rigid matrices at 77 K. Normal phosphorescence has not been observed from fluorenone triplet, and hence the emission spectra recorded both in solution at room temperature and in rigid matrices at 77 K have been assigned to fluorescence emission.[25,26] Fluorescence yield is increased significantly in rigid matrices at 77 K. However, we have made no attempt to determine the yield of fluorescence in rigid matrices because of the nonglassy nature of some of the matrices as well as the lack of knowledge regarding the exact path length of the sample.

Fluorescence maximum shows a large bathochromic shift in polar aprotic solvents, (e.g., acetonitrile and dimethylformamide (DMF)) as compared to that in a nonpolar solvent (e.g., cyclohexane). In solutions at room temperature, a fluorescence maximum appears at 470 nm in cyclohexane and at 515 nm in acetonitrile and DMF. This suggests a higher polarity or larger dipole moment of the S_1 state as compared to that of the ground state. The difference in dipole moment ($\Delta\mu$) between those of the S_1 state and the ground state has been determined by correlating the change in energy of the fluorescence maximum with the change in polarity of the cyclohexane−acetonitrile and benzene−acetonitrile solvent mixtures using the Lippert−Mataga equation.[46] The value of $\Delta\mu$ has been determined to be about 2.5 D. This value is a little higher than that (2.2 D) reported by the earlier authors.[43]

In each of the aprotic solvents, the fluorescence spectra recorded in solution and in rigid matrix at 77 K show neither any difference in shape nor any shift of the position of the maximum. However, in methanol (and other normal alcohols), the fluorescence spectra recorded in these two conditions are significantly different. The fluorescence spectrum recorded in solution has two distinct bands. One has a maximum at ca. 565 nm, and the other appear as a shoulder at ca. 514 nm. The position of the shoulder band coincides with the maximum of the fluorescence spectrum recorded in acetonitrile and DMF, either in solutions or in rigid matrices. However, the fluorescence spectrum recorded in the rigid matrix of methanol is characterized by a single band with a maximum at ca. 514 nm.

3.2. Picosecond Transient Absorption. Figure 3 shows the time-resolved transient absorption spectra recorded following photoexcitation of fluorenone in cyclohexane, acetonitrile, and

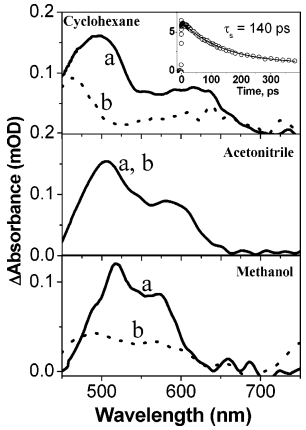

Figure 3. Transient absorption spectra of fluorenone recorded in cyclohexane, acetonitrile, and methanol at 0 ps (i.e., immediately after) (a) and at 6 ns (b) after photoexcitation using 355 nm laser pulses of 35 ps duration. Inset: temporal absorption profile recorded at 510 nm following photoexcitation of fluorenone in cyclohexane using 400 nm laser pulses of 70 fs duration. Solid line represents the best-fit single-exponential function.

methanol by 355 nm laser pulses of 35 ps duration. In cyclohexane and methanol, the transient spectra recorded immediately after the laser pulse (i.e., at 0 ps) and at 6 ns have been assigned to $S_n \leftarrow S_1$ and $T_n \leftarrow T_1$ absorptions, respectively, considering the values of the fluorescence lifetimes (0.14 ps and 2.1 ns in cyclohexane and methanol, respectively) reported earlier.[26,41] In acetonitrile, the fluorescence lifetime is about 19 ns.[26] Hence, we could not observe any kind of evolution of the absorption spectrum of the excited state in this solvent in the 6 ns time domain, and the spectrum is assigned to $S_n \leftarrow S_1$ absorption.

The absorption spectrum of the S_1 state recorded in each of the solvents studied here consists of two absorption bands in the 450−550 and 550−700 nm region. The maximum of the absorption band in the 450−550 nm region shows bathochromic shifts in more polar solvents. The maximum appears at 500, 510, and 525 nm in cyclohexane, acetonitrile, and methanol, respectively. On the other hand, the maximum of the absorption band in the 550−700 nm region shows a hypsochromic shift in the more polar solvent. In addition, the width of each of these bands narrows down significantly in acetonitrile and methanol as compared to that in cyclohexane.

3.3. Femtosecond Transient Absorption. Figure 4 shows the time-resolved absorption spectra of the transient species formed upon photoexcitation of fluorenone in acetonitrile and DMSO using 400 nm laser pulses of 70 fs duration. In each of these solvents, the absorption spectrum of the transient species formed immediately after the laser pulse consists of two main excited-state absorption (ESA) bands. In acetonitrile, these bands have the maxima at ca. 515 and 575 nm and shoulders at 490 and 610 nm. In DMSO, the maxima of the ESA bands are at ca. 490 and 540 nm and a shoulder at ca. 610 nm. In each of these solvents, the time-resolved transient absorption spectra recorded in sub-5 ps time domain reveal a slight decrease of absorbance in the 570−700 nm. Each of the temporal profiles recorded in this wavelength region consists of an ultrafast decay component, followed by another very long-lived component, which arises as a residual absorption in sub-500 ps time domain and can be assigned to the S_1 state. Two such typical temporal profiles recorded at 630 nm in acetonitrile and at 610 nm in DMSO are shown in the insets of Figure 4. The lifetimes of this short component are 1.4 ± 0.2 and 2.1 ± 0.2 ps in acetonitrile and DMSO, respectively.

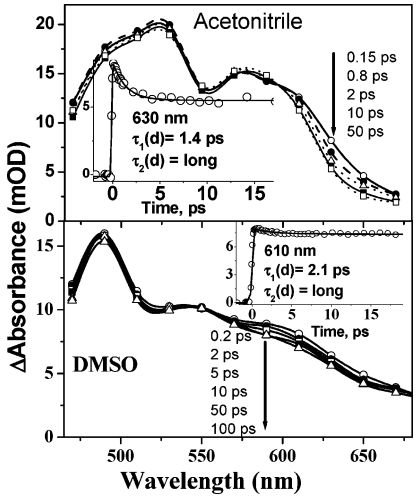

Figure 4. Time-resolved transient absorption spectra of fluorenone in acetonitrile and DMSO constructed for different delay times following photoexcitation with 400 nm laser pulses. Insets: temporal absorption profiles recorded at 630 and 610 nm following photoexcitation of fluorenone in acetonitrile and DMSO, respectively. Solid lines represent the best-fitted dual exponential functions. The lifetimes of the shorter component, which are given in the figure, are assigned to the vibrational energy relaxation process happening in the S_1 state and the long component arises due to long lifetime (∼19 ns) of the S_1 state of fluorenone in these solvents.

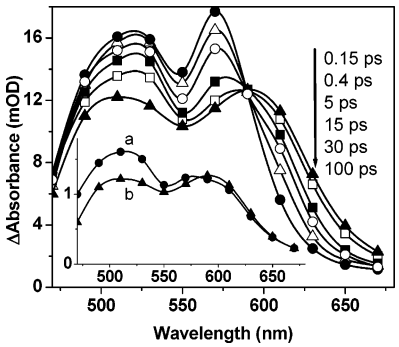

Figure 5. Time-resolved transient absorption spectra of fluorenone in 1-propanol, constructed for different delay times following photoexcitation using 400 nm laser pulses. Inset shows the comparison of the transient spectra constructed at 0.15 ps delay time following photoexcitation of fluorenone in acetonitrile (a) and 1-propanol (b).

Excited state relaxation dynamics of fluorenone has also been investigated in alcoholic solvents. The spectroscopic and the dynamical features of the transient species have been observed to be very similar in normal alcohols as well as in ethylene glycol. As a typical example, the time-resolved spectra of the transient species produced upon photoexcitation of fluorenone in 1-propanol using 400 nm laser pulses are shown in Figure 5. The transient spectrum constructed for the 0.15 ps delay time, i.e., immediately after photoexcitation, consists of two ESA bands with maxima at ca. 520 and 590 nm. These features are very similar to those of the transient spectrum, recorded in acetonitrile (inset of Figure 5), although the relative intensities of these two bands in these spectra are somewhat different. The features of the transient spectra evolve with increase in delay time because of decrease in absorbance in the 590−670 nm region and a concomitant increase in absorbance in the 490−590 nm region. As a result, we obtain a temporary near-isosbestic point at 590 nm. Following this spectral evolution, the transient absorption spectrum recorded at 100 ps has the absorption maxima at 515 and 570 nm. Further evolution of these ESA bands beyond the 500 ps time domain could not be

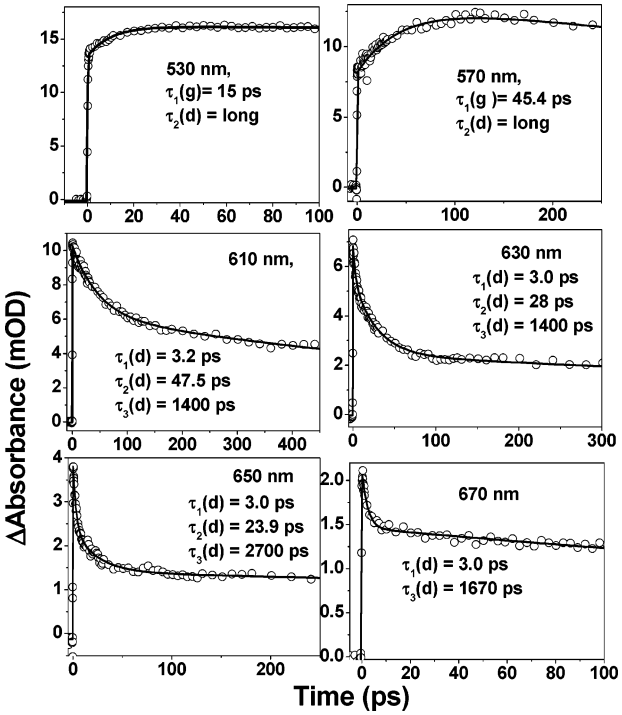

Figure 6. Temporal absorption profiles recorded at a few wavelengths following photoexcitation of fluorenone in 1-propanol using 400 nm laser pulses. Solid lines represent the best-fit two- or three-exponential functions. The lifetimes are also given in the figure. Since our spectrometer can record the profile up to about 500 ps delay time, the lifetime of the longest component cannot be determined accurately, but it only gives an indication of the presence of a ling-lived component due to the S_1 state of fluorenone.

followed using this spectrometer but could be followed using the picosecond spectrometer (Figure 3).

A few of the temporal profiles recorded at different wavelengths following photoexcitation of fluorenone in 1-propanol are presented in Figure 6, along with the multiexponential best-fit functions. The lifetimes associated with the corresponding fit functions are given in the figure as well as in Table 1 (the one with lifetime longer than 200 ps has not been given in this table). Since we can record the temporal profiles only up to about 550 ps delay time using our spectrometer, the lifetimes longer than 200 ps, which have been obtained from the fittings of the temporal profiles, do not provide an accurate value, but an indication of the presence of a longer-lived transient species. Each of the temporal profiles recorded in the 490−570 nm region shows an initial rise of transient absorption with the instrument response time (∼120 fs) followed by another slower growth. The growth lifetimes, τ_1(g), of the slower component have been determined at 510, 530, 550, and 570 nm. The values of τ(g), which have been obtained by analyzing the temporal profiles monitored at 510 and 530 nm, are seen to have nearly equal values (∼15 ± 0.5 ps) but are shorter than those obtained from the analyses of the profiles at 550 and 570 nm (45.4 ± 1 ps). However, the decay of the transient absorption after reaching the maximum following this growth monitored at each of these wavelengths is long (possibly longer than 1 ns).

In a series of normal alcoholic solvents, the viscosities of the solvents increase as the length of the linear hydrocarbon chain increases from methanol to 1-pentanol. The spectral and temporal characteristics of the transient species generated in these solvents as well as in ethylene glycol (EG) have been seen to be very similar to those in 1-propanol. To justify this, we have presented the temporal profiles recorded at a few selective wavelengths in EG solvent, which is the most viscous one among those used here (Figure 7). The values of the different lifetime components (except the one with lifetime longer than 200 ps) are also given in Table 1 for comparison of the values obtained from the analyses at different wavelengths as well as those obtained in different alcoholic solvents. This table shows that the values of τ(g), which are associated with the ESA bands with maxima at 515 and 570 nm, increase with increase in viscosity of the solvents. However, the trend of increasing the value of τ(g), associated with the ESA band with maximum at 515 nm, is not very regular with the viscosity of the solvents. Table 1 also shows that the values of τ_1(d), which have been obtained by fitting the temporal profiles recorded at 610, 630, 650, and 670 nm in each of the alcoholic solvents, are more or less independent of the monitoring wavelength. However, the value of τ_1(d) is nearly independent of the viscosity of the solvents; e.g., the values of τ_1(d) are 3.2 ± 0.2 and 2.7 ± 0.2 ps in methanol and EG, respectively. On the other hand, in a particular solvent, the value of τ_2(d) decreases with changing the monitoring wavelength from 610 to 670 nm. In a few cases, τ_2(d) is too short to distinguish from τ_1(d) at 650 or 670 nm. In all the alcoholic solvents, the value of τ_2(d) measured at 610 nm is nearly equal to the growth lifetime, τ_1(g), determined at 570 nm. Comparison of the values of τ_2(d), measured in different solvents but at the same monitoring wavelength, shows a regular increase with increase in viscosity of the solvent.

We have also investigated the relaxation dynamics of the S_1 state of fluorenone in TFE, which is a strong hydrogen bond donating solvent. The transient absorption spectrum constructed

TABLE 1: Lifetimes of the Transient Species, Which Have Been Determined at Different Wavelengths Following Photoexcitation of Fluorenone in Normal Alcoholic Solvents[a]

solvent	τ_D, ps;[b] τ_L, ps;[b] τ_{solv}, ps;[b] η, cP[c]	τ_1(g), ps (510/530 nm)	τ_1(g), ps (550/570 nm)	τ_1(d), ps, τ_2(d), ps (610 nm)	τ_1(d), ps, τ_2(d), ps (630 nm)	τ_1(d), ps, τ_2(d), ps (650 nm)
methanol	55.6; 9.2; 5, 0.54	5.7	16.3	3.0 21.7	3.2 19.5	3.3 14.7
ethanol	163; 27.4; 16, 1.08	12	36	3.2 33.6	3.0 25.2	3.0 22
1-propanol	329; 53, 26, 2.004	15	45.4	3.2 47.5	3.0 28	3.0 23.9
1-butanol	613; 120, 63, 2	36	50.5	3.0 50.5	3.1 41.5	3.0 35
1-pentanol	800; 151, 103, 3.6	23	58	3.0 59	2.7 41	2.8 24.5
ethylene glycol	813; 86, 15, 18	40	44	2.7 27.4	2.5 17.4	2.6

[a] The temporal profiles recorded at each of these wavelengths is associated with a long component having lifetime longer than 500 ps and cannot be determined accurately by our spectrometer, and hence these have not been put in this table. [b] Taken from refs 53 and 54. [c] Taken from ref 55. The viscosities are at 298 K.

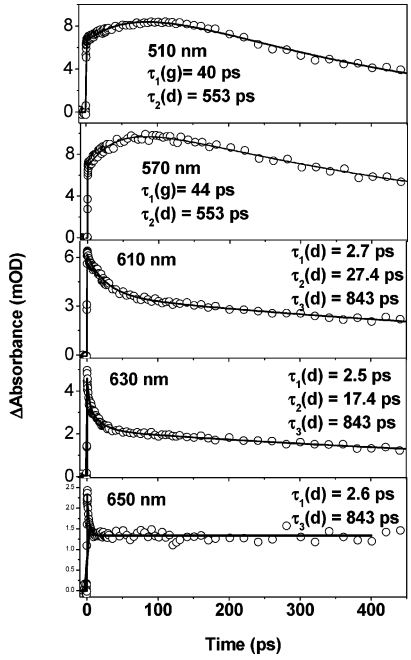

Figure 7. Temporal absorption profiles recorded at a few wavelengths following photoexcitation of fluorenone in ethylene glycol using 400 nm laser pulses. Solid lines represent the best-fit two- or three-exponential functions. The lifetimes are also given in the figure. Since our spectrometer cannot determine the lifetime of the longest component accurately, it gives only an indication of the presence of a ling-lived component due to the S_1 state of fluorenone.

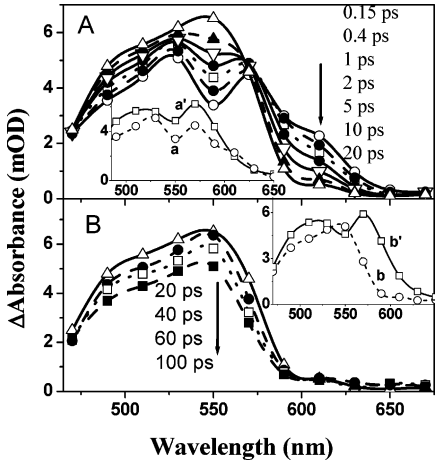

Figure 8. Time-resolved transient absorption spectra constructed for different delay times following photoexcitation fluorenone in TFE using 400 nm laser pulses. (A) Time-resolved spectrain sub-20 ps time domain. Inset of (A): comparison of the transient spectra constructed for 0.15 ps delay time in TFE (a) and in 1-propanol (a′). (B) Time-resolved spectra in post-20 ps time domain. Inset of (B): comparison of the transient spectra constructed for 100 ps delay time in TFE (b) and in 1-propanol (b′).

for 0.15 ps delay time consists of two ESA bands with maxima at 530 and 570 nm and shoulders at 490 and 610 nm (Figure 8). The spectral features are very similar to those of the spectrum recorded in 1-propanol at 0.15 ps delay time (inset of Figure 8A). Following the spectral evolution in sub-20 ps time domain, the transient spectrum constructed at 20 ps delay time is seen to consist of an ESA band with maximum at 550 nm and a shoulder at 510 nm. At longer delay times beyond 20 ps, this entire band decays without any further evolution of the spectral features. The features of the transient spectrum recorded at 20 ps delay time have been compared to those of the transient

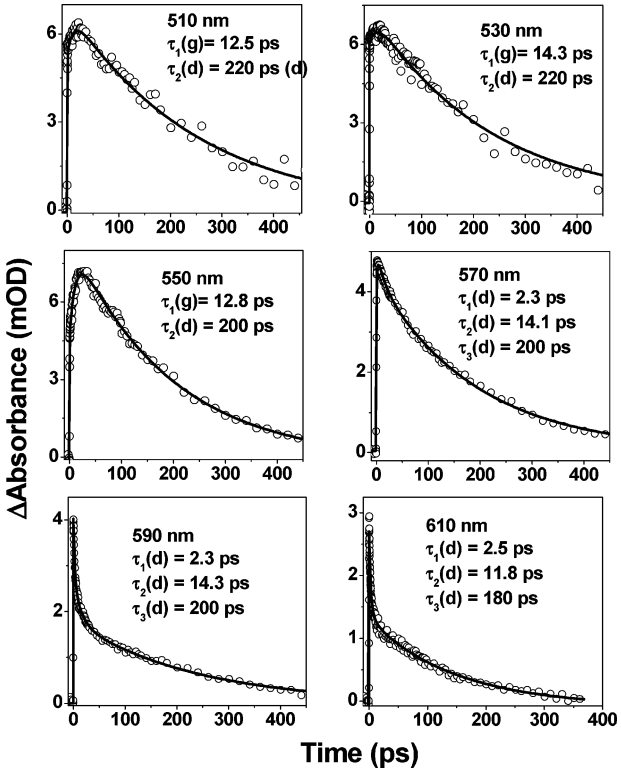

Figure 9. Temporal absorption profiles recorded at a few wavelengths following photoexcitation of fluorenone in TFE using 400 nm laser pulses. Solid lines represent the best-fit two- or three-exponential functions. The lifetimes are also given in the figure.

spectrum recorded at 100 ps delay time in 1-propanol (inset of Figure 8B). This shows that while the transient spectrum recorded in 1-propanol consists of two ESA bands with maxima at 520 and 570 nm, the transient spectrum recorded in TFE has only a single band with maximum at ca. 540 nm, and the band with maximum at 570 nm is missing in the later.

A few typical temporal profiles recorded in TFE are shown in Figure 9 along with the multiexponential best-fit functions. Like in other alcoholic solvents, the temporal profiles recorded at 510, 530, and 550 nm show the growth of a transient species with the instrument response time, followed by the growth of another transient species with the growth lifetime of 13.5 ± 1 ps. However, unlike in other alcohols, the growth lifetime is nearly independent of the monitoring wavelength in the 510−550 nm region. This suggests that in TFE we observe the formation of a single transient species. This fact is also supported by the similar decay lifetimes ($\tau_3 = 200 \pm 15$ ps) of this transient species determined at different monitoring wavelengths in the entire 490−590 nm region. In this solvent, the values of τ_2(d), measured at different wavelengths, are nearly equal.

3.4. Theoretical Study. To delineate the aspects of hydrogen bond dynamics in fluoreneone−alcohol systems investigated here, we have been motivated to study theoretically the fluorenone−methanol and fluorenone−TFE hydrogen-bonded complexes. For this purpose, ground-state geometries of these systems have been fully optimized (without any symmetry constraint) using different initial guess geometries. Calculations have been performed by density functional theory with B3LYP exchange-correlation methods using Gaussian basis set 6-31G*. All the calculations in this work have been done using the GAMESS electronic structure programs.[47]

In the ground state, we have been able to find two distinct conformations for the solute−solvent hydrogen-bonded complexes for both the fluorenone−methanol and fluorenone−TFE

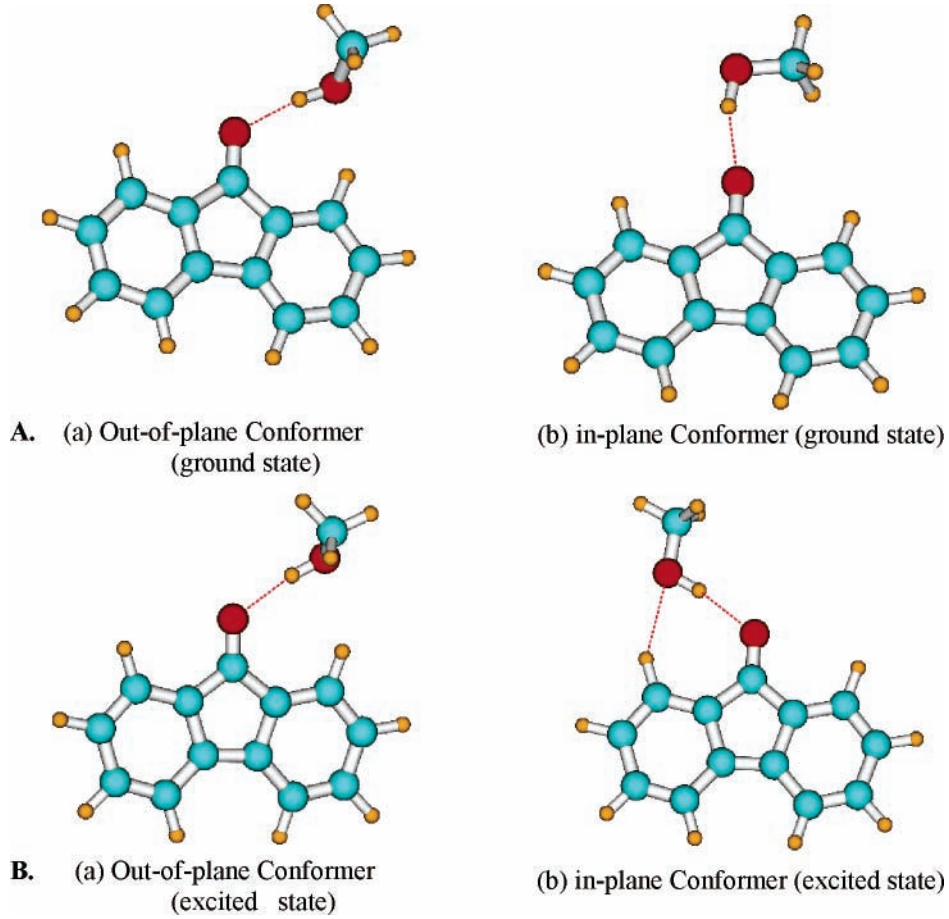

Figure 10. Optimized structures of the fluorenone−methyl alcohol hydrogen-bonded complexes in the ground state (A) and the relaxed S_1 state (B).

systems. The structures of these conformers have been presented in Figures 10A and 11A. Two different conformations have arisen because of the different orientations of the methyl or the trifluoroethyl group with respect to the plane on which the hydrogen bond (i.e., the [⟩C═O···H−O] moiety) exists. In both the conformations, the [⟩C═O···H−O] moiety remains on the plane of the fluorenone molecule. However, in one of the conformers of the fluorenone−methanol complexes, the carbon atom of the methyl group resides out of the plane. In this complex, the dihedral angle between the C−O bond of methanol and the [⟩C═O···H−O] moiety is −103°; i.e., the C−O bond is nearly perpendicular with respect to the [⟩C═O···H−O] moiety and the plane of the fluorenone molecule. We designate this form of the hydrogen-bonded complex as the "out-of-plane" conformer. Similarly, for the out-of-plane conformer of the fluorenone−TFE complex, the corresponding value of the dihedral angle is −54°. In other conformer, the C−O bond of the alcohol resides on the same plane as defined by the fluorenone molecule and the [⟩C═O···H−O] moiety. The dihedral angle between the [⟩C═O···H−O] moiety and the C−O bond is 179.9° and 179° for methanol and TFE complexes, respectively.We designate this form of the hydrogen-bonded complex as the "in-plane" conformer. It is to be noted that the ⟩C═O···H angle is about 122.3° in the out-of-plane structure, and the same has been calculated to be 169.7° for the in-plane structure of the methanol complexes. The corresponding values for the TFE complexes have been found to be 123.9° and 152.5°, respectively. The lengths of the hydrogen bonds have been found to be 1.909 and 1.960 Å for the out-of-plane and the in-plane conformations of the methanol complexes, respectively. The hydrogen bond energies for the methanol complexes have been calculated to be 38.3 and 23.2 kJ/mol for the out-of-plane and in-plane conformers, respectively. The corresponding values for the TFE complexes are 47.5 and 34.6 kJ/mol, respectively. Hence, the energy of the out-of-plane conformer is lower by 15.1 and 12.9 kJ/mol as compared to that of the in-plane conformer of the methanol and TFE complexes, respectively, which are in agreement with the corresponding hydrogen bond distances.

We also performed calculations to obtain the structures and the energetic of these hydrogen-bonded complexes in the S_1 state. In the FC state, the energy difference between these two conformers has been found to decrease to 10.7 and 8.3 kJ/mol for the methanol and TFE complexes as compared to those (15.1 and 12.9 kJ/mol) in the ground state.

We also made an attempt to obtain information about the geometry and energy of the relaxed S_1 states of the two conformers of the solute−solvent complexes. We optimized the geometries of the excited states using the configuration interaction singles (CIS) method.[48] In the relaxed S_1 state of the fluorenone−methanol complexes, both the conformers are found to be nearly isoenergetic with an energy difference of only 1.7 kJ/mol. While the hydrogen bond energy of the excited state of the out-of-plane conformer remains nearly the same (42.3 kJ/mol) as that of ground state, the same of the excited state of the in-plane conformer is increased to 40.6 kJ/mol. In the S_1 state of the in-plane conformation of the hydrogen-bonded complex, the methanol molecule reorients itself, residing on the same plane defined by the fluorenone molecule and [⟩C═O···H−O] moiety, to form the ⟩C−H···O hydrogen bond. Because

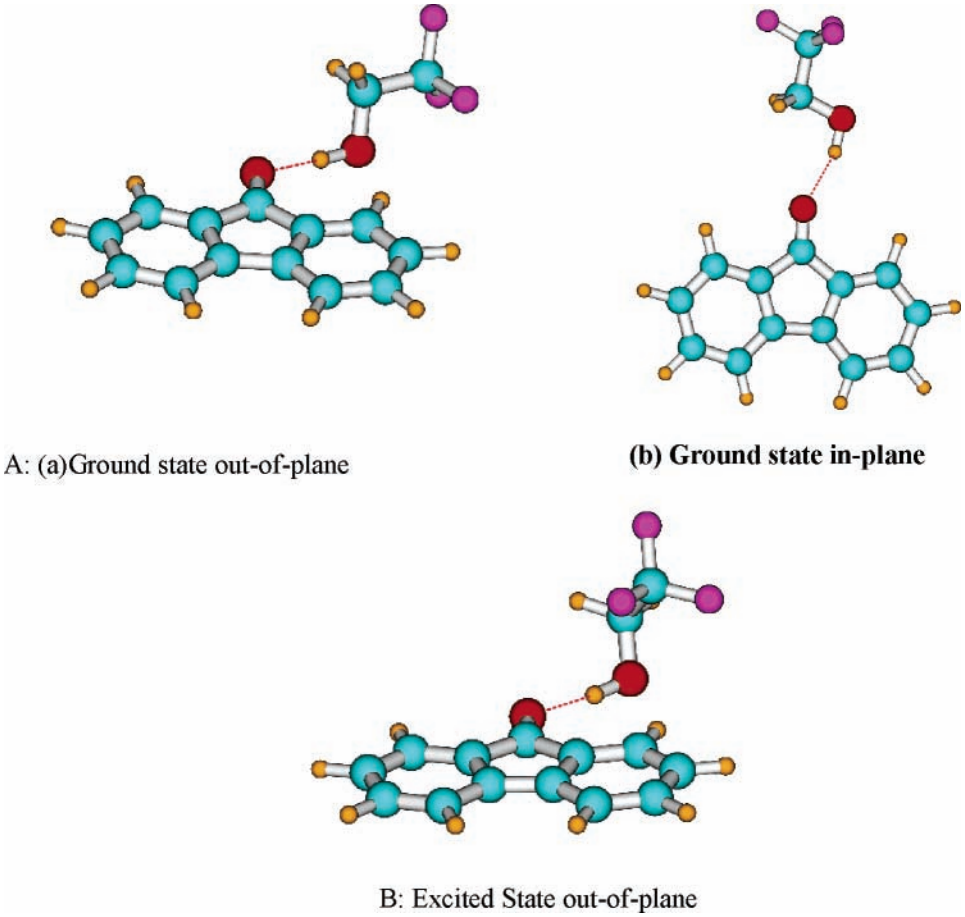

Figure 11. Optimized structures of the fluorenone−TFE hydrogen-bonded complexes in the ground state (A) and the relaxed S_1 state (B).

of the formation of this additional ⟩C−H···O hydrogen bond in the in-plane form, the energy difference between the two hydrogen-bonded species in the excited state is significantly reduced as compared to that in the ground state. It is also interesting to note that in the excited states the calculated lengths of the hydrogen bond are 1.903 and 1.896 Å for the out-of-plane and the in-plane conformers of the methanol complexes, respectively. In the excited state of the out-of-plane conformer, the C−O bond of the methanol molecule is found to be −72.9° with respect to the [⟩C═O···H−O] moiety. However, in the other conformer, the C−O bond resides on the same plane as that of the ⟩C═O···H−O moiety with a dihedral angle of nearly 0°. It is to be noted that the ⟩C═O···H angle is about 125.8° in the out-of-plane structure, and the same has been calculated to be 124.7° for the in-plane structure with a considerable deviation from the corresponding ground state value for the latter one. However, for the flurenone−TFE system we have been able to obtain only one conformer in the relaxed S_1 state, viz. out-of-plane conformer, although we have used the initial geometries of both in-plane and out-of-plane conformers. It is also interesting to note that in the excited states the calculated length of the hydrogen bond is 1.803 Å for this out-of-plane conformer of the complex. In this case the C−O bond of the methanol molecule is found to be −83.2° with respect to the [⟩C═O··· H−O] moiety. It is to be noted that the ⟩C═O···H angle is about 127.4° in this out-of-plane structure.

4. Discussion

4.1. Intermolecular Hydrogen-Bonding Interaction between Fluorenone and Alcohols. A careful examination of the effect of polarizability and hydrogen bond forming ability of the solvents on the positions and intensity of the individual absorption bands suggests that the excited electronic states corresponding to the 300−350 nm region are substantially different from those corresponding to the 270−300 and 350−500 nm regions. Fluorenone has been shown to form intermolecular hydrogen-bonded complex in the ground state with hydrogen bond donating alcohols.[35] We observe that the effect of hydrogen bond formation is more significant on the band in the 300−350 nm region than on those in other regions. Considering the fact that the effect of hydrogen bonding is more prominent on the absorption band in the 300−350 nm region than those in the 270−300 and 350−500 nm regions, it possibly can be concluded that the former band is associated with the transition involving the electronic orbitals centered on the carbonyl group and the latter ones are centered on the aromatic moiety. The equilibrium constants (K) for formation of the 1:1 complex with strong hydrogen-bonding solvents such as hexafluoropropanol (HFP) and TFE in methylene chloride have been determined to be 3.5 and 0.7 M^{-1}, respectively.[35] However, the normal alcohols are less effective in formation of complex in the ground state, and the values of K are much less than 0.6 M^{-1}.[35]

Fluorenone is very weakly fluorescent in solution at room temperature. Fluorescence yields (ϕ_F) of fluorenone have been reported to be 3.5×10^{-4}, 2.3×10^{-2}, and 1.1×10^{-3} in cyclohexane, acetonitrile, and ethanol, respectively.[26,41] A very low value of ϕ_F in cyclohexane suggests that the S_1 state has mixed $n\pi^*$ and $\pi\pi^*$ character due to energetic proximity of these two kinds of energy levels. This argument is supported by the fact that although the lifetime of the S_1 state is short, but much longer than that of a typical $n\pi^*$ kind of S_1 state in

benzophenone derivatives.[49] The lifetimes of the nπ^* kind of S_1 states in benzophenone and its derivatives are about 6−10 ps.[49,50] However, with increase in polarity, the $\pi\pi^*$ state, which lies above or near the nπ^* state on the energy scale in nonpolar solvents, comes down with respect to the latter and becomes the S_1 state in polar solvents, and both ϕ_F and τ_f values are increased by about 2 orders of magnitude in acetonitrile. In alcoholic solvents, despite the $\pi\pi^*$ character of the S_1 state, fluorescence is heavily quenched due to formation of the hydrogen-bonded complex.[35]

We observe dual-fluorescence behavior of fluorenone in solution of methanol (and other normal alcohols, too) at room temperature. The fluorescence spectrum consists of two emission bands with maxima at 514 and 565 nm, arising from the S_1 states of the non-hydrogen-bonded (or free) fluorenone molecules and the hydrogen-bonded complex, respectively. However, in rigid matrices at 77 K, we observe the presence of the only emission band arising from the excited state of free fluorenone molecules. This difference in the characteristics of the fluorescence spectra recorded in normal alcoholic solvents at two different conditions suggests that although the fluorenone molecules in the ground electronic state exist in equilibrium between the free fluorenone molecules and the hydrogen-bonded complex, the equilibrium remains strongly in favor of the free molecules. This is supported by the very low value of the equilibrium constant determined from the steady-state absorption experiments.[35] Since solvent relaxation is significantly slowed down or inhibited in rigid matrices at 77 K, we observe the only emission band with maximum at 514 nm, which arises from the excited state of the free fluorenone molecule. However, in solution at room temperature, we observe the appearance of both the emission bands, which are characteristics of the excited states of the free molecule and the hydrogen-bonded complex. The occurrence of the emission band arising from the hydrogen-bonded complex suggests the formation of the hydrogen bond between the S_1 state of fluorenone and the solvent by reorganization of the solvent molecules. Hence, comparison of the features of the steady-state fluorescence spectra of fluorenone in various kinds of media demonstrate that two spectroscopically distinct forms of fluorenone in the S_1 state are responsible for dual-fluorescence behavior of fluorenone in normal alcoholic solvents. Similar observations were made by Yoshihara and Kearns.[25] They could not assign the extra band of fluorescence emission with maximum at 565 nm in the spectrum recorded in solution to a species with a dimeric sandwich-type of arrangements or excimer emission but tried to interpret it as a "miscellaneous assortment of the solvent".

Assignment of the 565 nm fluorescence band to the hydrogen-bonded complex of the S_1 state of fluorenone is also supported by the fluorescence spectrum of fluorenone recorded in TFE at 77 K. Since TFE is a stronger hydrogen bond donating solvent as compared to methanol, the equilibrium constant for formation of the fluorenone−solvent hydrogen-bonded complex is larger in TFE than that in methanol.[35] Hence, in TFE, very few fluorenone molecules are left non-hydrogen-bonded in the ground state, and that is why we do not observe emission from the non-hydrogen-bonded species in the rigid matrix of TFE at 77 K. However, the fluorescence yield is negligibly small in TFE solution at room temperature because of efficient quenching of fluorescence due to hydrogen-bonding interaction with the solvent, and the spectrum could not be recorded.[35]

Assignment of the two fluorescence bands to the excited states of the free fluorenone molecule and the hydrogen-bonded complex has also been confirmed from the fluorescence spectra of fluorenone recorded in pure solvents and solvent mixtures of formamide and dimethyformamide. These two solvents have similar polarity on the π^* scale of solvent polarity, but formamide is a hydrogen bond donor while dimethylformamide is not.[51,52] In pure dimethylformamide, the fluorescence maximum appears at 514 nm, which is due to the emission from the free form. Although, unlike the spectra in alcoholic solvents, the bands due to the free molecule and the hydrogen-bonded complex are not resolved, the broadening and shifting characteristics of the new spectral component due to the hydrogen-bonded form with increasing concentration of formamide are apparent. The fluorescence spectrum with a maximum at 562 nm recorded in pure solvent of formamide suggests that emission from the hydrogen-bonded complex has a significant contribution to the total emission.

4.2. Vibrational Energy Relaxation. We observe that in all kinds of solvents the decay of transient absorption monitored in the 610−670 nm region following photoexcitation of fluorenone using 400 nm light is associated with an ultrafast component with lifetime τ_1(d), varying in the range 1.4−3.2 ps. Since the lifetime of the S_1 state of fluorenone in acetonitrile is about 19 ns,[41] ultrafast evolution of the spectral characteristics in aprotic solvents must be considered to be happening in the Franck−Condon region of the potential energy surface. The ultrafast decay lifetimes of the transient absorption may be considered to be arising because of either of the following two processes, namely, solvation of the relatively more polar S_1 state or solvent-induced vibrational energy relaxationn (VER) process that is caused by elastic or quasielastic collisions between the solute and solvent molecules.[20,21] However, we mentioned earlier that the change in dipole moment of the fluorenone molecule due to photoexcitation is not large ($\Delta\mu \sim 2.5$ D). Additionally, the time constant (i.e., 1.4 ps) associated with the evolution of the time-resolved spectra in acetonitrile is much slower than the solvation time of this solvent ($\tau_{solv} \sim 0.3-0.7$ ps).[6,53,54] The value of τ_1(d) in alcoholic solvents also does not have any correlation with the solvation time (Table 1). Hence, the process associated with these time constants cannot be assigned to the solvation phenomenon. On the other hand, we calculate that the energy of the zero vibrational level of the S_1 state of fluorenone in acetonitrile (from the intersection point of the normalized absorption and fluorescence spectra of fluorenone) is 22 400 cm^{-1}. Hence, it becomes evident that the excitation of fluorenone with a photon of 400 nm wavelength (energy of a photon is 25 000 cm^{-1}) creates the molecules in a vibrational level, which lies at about 2728 cm^{-1} higher in energy than the zero vibrational level of the S_1 state. Considering a rigid and simple chemical structure of fluorenone, the ultrafast time constants τ_1(d) can only be correlated to a process in which the vibrationally hot molecules in the S_1 state transfer the excess vibrational energy to the surrounding solvent molecules.[20,21]

Variation of τ_1(d) with the change in the characteristics of the solvents is not very significant and cannot be correlated with the change in viscosities of the solvents. For example, DMSO is 6 times more viscous than acetonitrile, but τ_1(d) increases marginally in the case of DMSO (2.4 ps) as compared to that in acetonitrile (1.4 ps). Again, EG is about 30 times more viscous than methanol, but τ_1(d) (2.7 ps) in EG is shorter than that in methanol (3.2 ps). However, the small variation of τ_{vib} can possibly be correlated with the dipole moment (μ) of the solvents. Normal alcohols, such as methanol ($\mu = 1.7$ D), ethanol ($\mu = 1.7$ D), and 1-butanol ($\mu = 1.8$ D), have nearly the same dipole moments,[55] and hence τ_1(d) has nearly the same values (τ_1(d) = 3.1 ± 0.1 ps) in these solvents. The dipole

moment of EG is 2.3 D, and τ_1(d) has a lower value (2.7 ps). The value of τ_1(d) (2.5 ps) is further lowered in TFE, which is more polar (we do not know the dipole moment value for this solvent) than the other alcoholic solvents. Hence, this shows that the lifetime of the VER process has lower value in hydrogen-bond-donating solvents of higher polarity. In the excited state of fluorenone, the dipole moment of fluorenone is about 6 D (since $\mu_e - \mu_g = 2.5$ D and $\mu_g = 3.35$ D[56]), and hence the C═O group is expected to have a reasonably high charge density because of an intramolecular charge-transfer character of the S_1 state. Electrostatic coupling between the C═O stretching vibration with the intermolecular modes of the solvents, possibly via the hydrogen bond stretching vibration, modulate the solvent dipole moment density, and this coupling is mainly responsible for the ultrafast vibrational energy relaxation process in the S_1 state. In aprotic solvents, however, the trend is reverse. The value of τ_1(d) is larger in DMSO ($\mu = 4.1$ D) than that in acetonitrile ($\mu = 3.5$ D).[55] We are not able to explain this trend.

4.3. Hydrogen Bond Dynamics. Our steady-state fluorescence spectroscopic study has clearly revealed that in solutions of fluorenone in normal alcoholic solvents both the free fluorenone molecule and the hydrogen-bonded complex exist in equilibrium, although the equilibrium remains in favor of the free molecule. However, in TFE, which is a strong hydrogen-bond-donating solvent, the equilibrium shifts in favor of the hydrogen-bonded complex. Hence, photoexcitation of fluorenone molecules in solutions of normal alcoholic solvents using 400 nm laser light creates the excited states of both the free fluorenone molecule as well as its hydrogen-bonded complex. On the other hand, in TFE, we expect to create the excited state of only the hydrogen-bonded complex.

Considering the similar positions of the maxima in the transient spectra recorded at 0.15 ps delay time in acetonitrile and 1-propanol (inset of Figure 5), the transient spectrum in 1-propanol may be assigned to the excited state of the free form of fluorenone. This might have been formed either upon photoexcitation of the free fluorenone molecule existing in the ground state or ultrafast photodissociation of the hydrogen bond in the excited state of the hydrogen-bonded complex. Similarities in the features of the transient spectrum recorded at 0.15 ps delay time in 1-propanol and TFE (Figure 8) too support the fact that upon photoexcitation the hydrogen-bonded complex dissociates easily and rapidly, and the excited state of the free fluorenone molecule is produced in an ultrafast time scale (which is faster than the time resolution of our spectrometer). However, the solvent molecules cannot reorganize rapidly to incorporate the newly released alcohol molecule into its two-dimensional hydrogen bond network structure; i.e., there is a "dangling" hydrogen bond still present.[24] This nonequilibrated state of the excited fluorenone molecule is associated with a completely non-hydrogen-bonded solvent molecule, or a solvent molecule bonded into a chain to form a branch point, or some other unfavorable hydrogen bond configuration. This is a poorly solvated state, which is sufficiently unstable and tends to undergo geminate re-formation of fluorenone−alcohol hydrogen bond with high probability. This re-formation process is accompanied by the requisite reorganization of the hydrogen bond structure of the solvent to fully equilibrate and incorporate the dangling hydrogen bond into the hydrogen bond network structure of the solvent. With increase in delay time, the evolution of the time-resolved absorption spectra, which is associated with the rapid decrease of transient absorption in the 590−700 nm region and concomitant increase in absorption in the 510−590 nm region, can be assigned to the geminate re-formation of the hydrogen bond possibly with a new equilibrium geometry, accompanied by equilibration of the hydrogen bond network structure of the solvent.

Comparing the features of the time-resolved spectra recorded in acetonitrile (Figure 4), 1-propanol (Figure 5), and TFE (Figure 8), we find that, although in all three cases we observe the decrease of absorbance in the 610−670 nm region, the change is more significant in the case of 1-propanol and TFE. In addition, we observe a concomitant increase of transient absorption in the 470−590 nm region, resulting the development of new and distinct ESA bands in alcoholic solvents. However, it is important to note that 1-propanol (dielectric constant, $\epsilon \sim 21.1$) is less polar than acetonitrile ($\epsilon \sim 38$). Hence, the significant difference in evolution of the spectral characteristics of the transient species in these two solvents cannot be assigned to the simple dipolar solvation but obviously to the hydrogen-bonding interaction between the excited state of fluorenone and the solvent. In other words, the hydrogen bond dynamics is responsible for the observed evolution of the time-resolved spectra of the S_1 state of fluorenone in alcohols. The occurrence of the temporary isosbestic points at 590 and 570 nm in the time-resolved spectra recorded in 1-propanol and TFE, respectively, apparently suggests the involvement of two different excited states, one of which is the excited state of the free fluorenone molecule and the other is the excited state of the hydrogen-bonded complex. (The occurrence of the isosbestic point in 1-propanol is possibly fortuitous; vide infra.) The occurrence of the isosbestic point is also an important indicator, in particular, to suggest that the evolution of the time-resolved transient absorption spectrum in alcohols is not associated with a dipolar solvation process, which is associated with the reorientation of the solvent dipoles in response to the electronic charge reorganization in the solute due to creation of the excited state. The dipolar solvation process is normally revealed by the evolution of the continuum of states.

We assign both the growth lifetime, τ_1(g), of the ESA measured in the 510−550 nm region and the decay lifetime, τ_2(d), measured in the 570−610 nm region (τ_1(g) = τ_2(d) = 12.5 ± 2 ps, as shown in Figure 9) to the geminate re-formation of the hydrogen-bonded complex in the excited state, accompanied by the equilibration of the hydrogen bond network structure of the solvent, TFE. The decay lifetime component, τ_3(d) = 200 ± 15 ps, is assigned to the decay of the excited state of the fluorenone−TFE hydrogen-bonded complex. In normal alcohols, the excited state of the free fluorenone molecule, which is created by photodissociation of the hydrogen-bonded complex in the excited state, undergoes geminate re-formation of the hydrogen bond. On the other hand, the excited state of the free fluorenone molecule, which is created upon photoexcitation of the molecule in the ground state, undergoes hydrogen bond formation as well because of larger polarity of the excited state. Development of two ESA bands with maxima at 515 and 570 nm with different growth lifetimes, as well as the wavelength-dependent decay of the excited state of the non-hydrogen-bonded form measured in the 610−650 nm region, is possibly the consequence of formation of two different conformers of the hydrogen-bonded complex in the excited state (Figures 5 and 6). Results of our theoretical calculation support the experimental observation that, in normal alcoholic solvents, two different kinds of hydrogen-bonded complex with different orientations of the hydrogen bond are formed in the excited state of fluorenone. Hence, it becomes obvious that the occurrence of the temporary isosbestic point at 590 nm in the

time-resolved spectra recorded in 1-propanol (Figure 5) is really fortuitous. On the other hand, the experimental revelation regarding the formation of only one kind of hydrogen-bonded complex in the S_1 state of fluorenone in TFE has also been supported by our calculation. In addition, our calculation also reveals that the geometries of the hydrogen-bonded species in the relaxed S_1 state are significantly different from that in the ground state. This supports our experimental findings that following photoexcitation the relaxation of the excited fluorenone molecule should involve repositioning of the hydrogen bonds.

4.4. Hydrogen Bond Dynamics vs Solvation. The standard picture of nonspecific solvation dynamics assumes relatively weak intermolecular interactions between the excited solute and the surrounding solvent molecules. The nature of interaction between the solute and each of the large number of solvent molecules is equally important, and the dynamics is associated with the motion of many solvent molecules along a collective coordinate. The barriers to these motions are small compared to thermal energies. However, although the energy barrier for the hydrogen bond breaking or forming is low, but not negligible as compared to the thermal energies. In reality, hydrogen-bond dynamics is intermediate between nonspecific solvation and covalent bond breaking.[24] Interaction of the solute with the single hydrogen-bonded solvent molecule is stronger than its interaction with other solvent molecules. However, the strength and dynamics of this interaction may not be too much different from the hydrogen bond interaction between the solvent molecules, and hence the latter may influence the relaxation dynamics of the excited solute molecule in a significant way. Because of the intermediate strength of the hydrogen bond, it is not clear which picture should be more appropriate. Our experimental measurements possibly show the features, which are characteristic of both. In the present case, while the hydrogen bond dynamics investigated in TFE can be thought of a bond-breaking and bond-making chemical reaction rather than a solvation process, in normal alcohols, the wavelength-dependent dynamics of the hydrogen bond leads us to consider it as merely a solvation process.

In hydrogen-bonding solvents, the longest component of the Debye dielectric relaxation time is generally assumed to be connected with the rate of hydrogen bond reorganization in the solvent; i.e., the growth lifetimes, $\tau_1(g)$, should be proportional to the Debye relaxation time (τ_D) and longitudinal relaxation times (τ_L) of the solvents (eqs 1 and 2).[57, 58]

$$\tau_1(g) = A(\tau_{D,L}) \exp(\Delta H/RT) \quad (1)$$

$$\ln(\tau_1(g)) = \ln(\tau_{D,L}) + A + (\Delta H/RT) \quad (2)$$

If we assume that the Arrhenius parameter, ΔH, does not vary significantly due to change of solvents of the same class, we expect a linear relation between $\ln(\tau_1(g))$ and $\ln(\eta)$ (eq 2). Figure 12 shows that both the sets of values of $\tau_1(g)$ (Table 1), which provides the correlation time for hydrogen bond dynamics in the corresponding solvent, are well correlated with both τ_D and τ_L. We also observe good correlation between $\tau_1(g)$ and the rotational correlation times (τ_R) for the OH group in methanol (5 ps), ethanol (18 ps), and 1-propanol (33 ps), obtained from NMR measurements.[59] However, it is important to note that, although we see a good correlation between $\tau_1(g)$ and τ_D, τ_L, or τ_R, the absolute values of these parameters do not match exactly with τ_g. Here, it should be realized that reorientation, as it is measured in the Debye relaxation and in the rotational correlation experiments, and thermalization are not the same process. The repositioning of the molecules in a thermalization process mainly involves a change of distance between the molecules, e.g., hydrogen bond lengths. Recently, the hydrogen bond dynamics has been studied for liquid water.[60] The correlation time constant of the hydrogen bond length was observed to be ~500 fs, whereas τ_D and τ_R values for water are 8 and 2.6 ps, respectively. From this comparison of the time scales, it is clear that the modulation of hydrogen-bond length is a faster process than the orientation of the molecules. Hence, it is not surprising that because of the involvement of the thermalization process, the equilibration time of hydrogen bond measured here are shorter than the Debye relaxation time.[61]

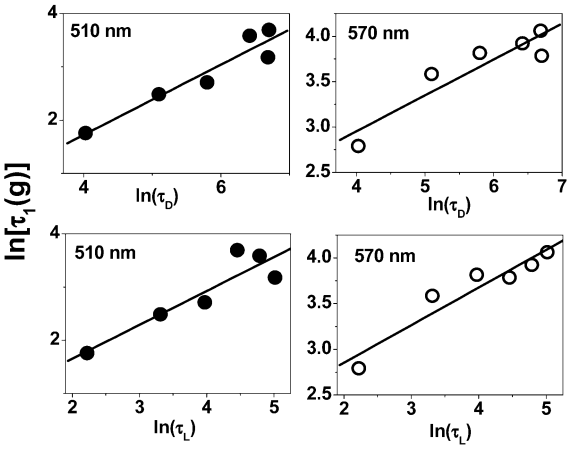

Figure 12. Correlation between the growth lifetimes, $\tau_1(g)$, monitored at 510 and 570 nm with the Debye relaxation times, τ_D, and the longitudinal relaxation times, τ_L, of the alcoholic solvents.

5. Conclusion

Steady-state absorption and fluorescence spectroscopic behavior of fluorenone have been investigated in various kinds of media, such as protic and aprotic solvents of different polarity at room temperature as well as in solid matrices at 77 K. A comparison of these spectra establishes the fact that two spectroscopically distinct forms of fluorenone exist in the S_1 state, namely, the non-hydrogen-bonded (or free) molecule as well as the hydrogen-bonded complex, which are responsible for the dual-fluorescence behavior of fluorenone in solutions of normal alcoholic solvents at room temperature (298 K). However, in 2,2,2-trifluoroethanol, a strong hydrogen bond donating solvent, emission from only the hydrogen bonded complex is observed. The time-resolved transient absorption measurements have been performed following photoexcitation of fluorenone in both polar aprotic solvents and polar protic solvents using 400 nm laser pulses. These measurements reveal, in addition to a long residual component (lifetime of which is longer than 1 ns and assigned to that of the S_1 state), the presence of an ultrafast component, which has been assigned to the solvent-induced vibrational energy relaxation (VER) process. However, in alcoholic solvents, in addition to the VER process, significant evolution of the spectroscopic and dynamical properties of the S_1 state has been observed because of repositioning of the hydrogen bonds around the carbonyl group. In alcoholic solvents, the ground state of fluorenone exists in equilibrium between the free molecule and the hydrogen-bonded complex form. Upon photoexcitation of fluorenone in alcoholic solvents, both the forms are excited. However, the hydrogen-bonded complex undergoes photodissociation quickly. Hence, immediately after photoexcitation, only the non-hydrogen-bonded form exists, and it undergoes formation and geminate re-

formation of the hydrogen bond. These processes are also accompanied by the reorganization of the two-dimensional hydrogen bond network structure of the solvent. The growth lifetime of the hydrogen-bonded complex has been assigned to the equilibration time for the hydrogen bond in the excited state of fluorenone in alcohols. Time-resolved spectra and the wavelength-dependent temporal dynamics investigated in normal alcohols reveal the existence of two different kinds of hydrogen-bonded complex of the fluorenone−alcohol system with different orientations of the hydrogen bond with respect to the carbonyl group and the molecular plane of fluorenone. On the other hand, the time-resolved measurements in 2,2,2-trifluoroethanol (TFE) indicate the formation of only one kind of hydrogen-bonded complex. To delineate these aspects, we performed theoretical calculations to find out energetic and the geometrical conformations of the fluorenone−methanol and fluorenone−TFE hydrogen-bonded complexes, in both the ground and the excited states. Truly, we have been able to find two distinct conformations, e.g., in-plane and out-of-plane, for the fluorenone−methanol complexes, but only the out-of-plane conformation for the fluorenone−TFE complex in the excited state of fluorenone. We find a linear correlation between the lifetimes of the equilibration process occurring because of repositioning of the hydrogen bonds and Debye or longitudinal relaxation times of the normal alcoholic solvents. This establishes the fact that in weakly hydrogen bond donating solvents the hydrogen bond dynamics can be described as merely a solvation process. Whereas, in strong hydrogen-bond-donating solvents, such as TFE, hydrogen bond dynamics can be better described by a process of conversion between two distinct excited states, namely, the free molecule and the hydrogen-bonded complex.

Acknowledgment. The authors are grateful to Dr. T. Mukherjee, Associate Director, Chemistry Group, BARC, for his constant encouragement.

References and Notes

(1) Perrin, C. L.; Nielson, J. B. *Annu. Rev. Phys. Chem.* **1997**, *48*, 511.
(2) *Hydrogen-Bonded Liquids*; Dore, J. C., Teixira, J., Eds.; Kluwer Academic: Boston, 1991.
(3) Pimental, G. C.; McClellan, A. L. *Annu. Rev. Phys. Chem.* **1971**, *22*, 347.
(4) Schuster, P., Zundel, G., Sandorfy, C., Eds. *The Hydrogen Bond: Recent Developments in Theory and Experiments*; North-Holland: Amsterdam, 1976.
(5) Maroncelli, M.; MacInnis, J.; Fleming, G. R. *Science* **1989**, *243*, 1674.
(6) Maroncelli, M. *J. Mol. Liq.* **1993**, *57*, 1.
(7) Barbara, P. F.; Jarzeba, W. *Adv. Photochem.* **1990**, *15*, 1.
(8) Barthel, E. R.; Martini, I. B.; Keszei, E.; Schwartz, B. J. *J. Chem. Phys.* **2003**, *118*, 5916.
(9) Jimenez, R.; Fleming, G. R.; Kumar, P. V.; Maroncelli, M. *Nature (London)* **1994**, *369*, 471.
(10) Pant, P.; Riter, R. E.; Levinger, N. E. *J. Chem. Phys.* **1998**, *109*, 9995.
(11) Luzar, A.; Chandler, D. *Nature (London)* **1996**, *379*, 5.
(12) Woutersen, S.; Emmerichs, U.; Baker, H. J. *Science* **1997**, *278*, 658.
(13) (a) Chudoba, C.; Nibbering, E. T. J.; Elsaesser, T. *Phys. Rev. Lett.* **1998**, *81*, 3010. (b) Chudoba, C.; Nibbering, E. T. J.; Elsaesser, T. *J. Phys. Chem. A* **1999**, *103*, 5625.
(14) Palit, D. K.; Zhang, T.; Kumazaki, S.; Yoshihara, K. *J. Phys. Chem. A* **2003**, *107*, 10788.
(15) Kwok, W. M.; George, M. W.; Grills, D. C.; Ma, C.; Matousek, P.; Parker, A. W.; Phillips, D.; Toner, W. T.; Towrie, M. *Angew. Chem., Int. Ed.* **2003**, *42*, 1826.
(16) *Ultrafast Reaction Dynamics and Solvent Effects*; Gauduel, Y., Rosky, P. J., Eds.; American Institute of Physics: New York, 1994.
(17) *Ultrafast Dynamics of Chemical Systems*; Simon, J. D., Ed.; Kluwer Academic Publishers: Dordrecht, 1994.
(18) *Femtochemistry and Femtobiology: Ultrafast Reaction Dynamics at Atomic Scale Resolution*; Sundström, V., Ed.; Imperial College Press: London, 1996.
(19) Elsaesser, T.; Kaiser, W. *Annu. Rev. Phys. Chem.* **1991**, *42*, 83.
(20) Owrutsky, J. C.; Raftery, D.; Hochstrasser, R. M. *Annu. Rev. Phys. Chem.* **1994**, *45*, 519.
(21) Martini, I.; Hartland, G. V. *J. Phys. Chem.* **1996**, *100*, 19764.
(22) Grabowski, Z. R.; Rotkiewicz, K.; Rettig, W. *Chem. Rev.* **2003**, *103*, 3857.
(23) Glasbeek, M.; Zhang, H. *Chem. Rev.* **2004**, *104*, 1929.
(24) Benigno, A. J.; Ahmed, E.; Berg, M. *J. Chem. Phys.* **1996**, *104*, 7382.
(25) Yoshihara, K.; Kearns, D. R. *J. Chem. Phys.* **1966**, *45*, 1991.
(26) Biczok, L.; Berces, T.; Marta, F. *J. Phys. Chem.* **1993**, *97*, 8895.
(27) Kobayashi, T.; Nagakura, S. *Chem. Phys. Lett.* **1976**, *43*, 429.
(28) Biczok, L.; Berces, T. *J. Phys. Chem.* **1988**, *92*, 3842.
(29) Greene, B. I.; Hochstrasser, R. M.; Weisman, R. B. *J. Chem. Phys.* **1979**, *70*, 1247.
(30) Andrews, L. J.; Deroulede, A.; Lanschitz, H. *J. Phys. Chem.* **1978**, *82*, 2304.
(31) Singer, L. A. *Tetrahedron Lett.* **1969**, 923.
(32) Caldwell, R. A. *Tetrahedron Lett.* **1969**, 2121.
(33) Gutten plan, J. B.; Cohen, S. G. *Tetrahedron Lett.* **1969**, 2125.
(34) Caldwell, R. A.; Gajewski, R. P. *J. Am. Chem. Soc.* **1971**, *93*, 533.
(35) Biczok, L.; Berces, T.; Linschitz, H. *J. Am. Chem. Soc.* **1997**, *119*, 11071.
(36) Turro, N. J. *Modern Molecular Photochemistry*; Benjamin/Cumings: Menlo Park, CA, 1978; Chapter 6.
(37) Mataga, N.; Kubota, T. *Molecular Interactions and Electronic Spectra*; Dekker: New York, 1970; Chapters 7 and 8.
(38) El-Sayed, M. A. *J. Chem. Phys.* **1962**, *36*, 573; **1963**, *38*, 2834.
(39) Heldt, J. R.; Heldt, J.; Jozefowicz, M.; Kaminski, J. *J. Fluoresc.* **2001**, *11*, 65.
(40) Davis, G. A.; Carapelluci, Szoc, K.; Gresser, J. D. *J. Am. Chem. Soc.* **1969**, *91*, 2264.
(41) Yatuhashi, T.; Nakajima, Y.; Shimada, T.; Inoue, H. *J. Phys. Chem. A* **1998**, *102*, 3018.
(42) Jozefowicz, M.; Heldt, J. R. *Chem. Phys.* **2003**, *294*, 105.
(43) Liptay, W.; Weissenbergger, H.; Tiemann, F.; Eberlein, W.; Konopka, G. *Z. Naturforsch., A* **1968**, *23*, 377.
(44) Singh, A. K.; Bhasikuttan, A. C.; Palit, D. K.; Mittal, J. P. *J. Phys. Chem. A* **2000**, *104*, 7002.
(45) Kuboyama, A. *Bull. Chem. Soc. Jpn.* **1964**, *37*, 1540.
(46) (a) Lippert, E. *Z. Naturforsch.* **1955**, *10A*, 541. (b) Mataga, N.; Kaifu, Y.; Koizumi, M. *Bull. Chem. Soc. Jpn.* **1955**, *28*, 690.
(47) Schmidt, M. W.; BalDridge, K. K.; Boatz, J. A.; Elbert, S. T.; Gordon, M. S.; Jensen, J. H.; Koseki, S.; Matsunaga, N.; Nguyen, K. A.; Su, S. J.; Windus, T. L.; Dupuis, M.; Montgomery, J. A., Jr. *J. Comput. Chem.* **1993**, *14*, 1347.
(48) Foresman, J. B.; Head-Gordon, M.; Pople, J. A.; Frisch, M. J. *J. Phys. Chem.* **1992**, *96*, 135−149.
(49) (a) Miyasaka, H.; Morita, K.; Kamada, K.; Mataga, N. *Bull. Chem. Soc. Jpn.* **1990**, *63*, 3385. (b) Suter, G. W.; Wild, U. P.; Schaffner, K. *J. Phys. Chem.* **1986**, *90*, 2558. (c) Prater, K.; Freund, W. L.; Bowman, R. M. *Chem. Phys. Lett.* **1998**, *295*, 82.
(50) Singh, A. K.; Bhasikuttan, A. C.; Palit, D. K.; Mittal, J. P. *J. Phys. Chem. A* **2000**, *104*, 7002.
(51) Reicherdt, C. *Solvents and Solvent Effects in Organic Chemistry*; VCH Verlagsgesellschaft GmbH: FRG, 1990.
(52) (a) Kamlet, J. M.; Abboud, J. L.; Taft, R. W. *J. Am. Chem. Soc.* **1977**, *99*, 6027. (b) Kamlet, J. M.; Abboud, J. L.; Taft, R. W. *Prog. Phys. Org. Chem.* **1981**, *13*, 485.
(53) Simon, J. D. *Acc. Chem. Res.* **1988**, *21*, 128.
(54) Horng, H. L.; Dahl, K.; Jones, G., II; Maroncelli, M. *Chem. Phys. Lett.* **1999**, *315*, 363.
(55) Riddick, J. A.; Bunger, W. B. *Organic Solvents*, 3rd ed.; Wiley: New York, 1970.
(56) Fessenden, R. W.; Shimamori, H.; Scaianao, J. C. *J. Phys. Chem.* **1982**, *86*, 3803.
(57) Bertolini, D.; Cassettari, M.; Salvetti, G. *J. Chem. Phys.* **1982**, *76*, 325.
(58) Garg, S. K.; Smyth, C. P. *J. Phys. Chem.* **1965**, *69*, 1294.
(59) Ludwig, R.; Zeidler, M. D. *Mol. Phys.* **1966**, *10*, 451.
(60) (a) Gale, G. M.; Gallot, G.; Hache, F.; Lascoux, N.; Bratos, S.; Leicknam, J.-C. *Phys. Rev. Lett.* **1999**, *82*, 1086. (b) Woutersen, S.; Bakker, H. J. *Phys. Rev. lett.* **1999**, *83*, 2707.
(61) Lock, A. J.; Woutersen, S.; Bakker, H. J. *J. Phys. Chem. A* **2001**, *105*, 1238.